An Energy Based Two Level Prioritized Control for Virtual Humans

Mingxing Liu, Alain Micaelli, Paul Evrard, Adrien Escande, and Claude Andriot
CEA, LIST, Interactive Simulation Laboratory,
18 route du Panorama, BP6,
FONTENAY AUX ROSES, F- 92265 France
Email: {mingxing.liu, alain.micaelli, paul.evrard, adrien.escande, claude.andriot}@cea.fr

Abstract— This paper presents an approach to address conflicting motion tasks in multi-objective control of virtual humans. The novelty in our approach is that we can handle the inequality constraints and maintain the passivity as well. The targets associated with lower priority tasks are constrained so as to guarantee that the higher priority tasks can be sufficiently fulfilled. The multi-objective controller takes as inputs the desired task targets and computes the optimal task wrenches by solving an optimization problem. Finally, the joint torques are computed according to the optimal task wrenches. This control approach can be realized in real-time. Simulations demonstrate that the proposed method can improve the behavior of a virtual human.

Index Terms— Motion control, Prioritization, Multi objective control, Virtual human, Passivity.

I. INTRODUCTION

Virtual humans will become more and more useful in training environments and in industry design. In these applications, a virtual human (VH) is often required to perform multiple tasks simultaneously, where a task means that a certain frame on the VH's body should be transferred from an initial state to a desired state. For example, we can define a task for the center of mass (CoM) for balance control, or tasks for the end-effectors for motion tracking control. In a physics simulation environment, a VH body can be considered as a mechanical system influenced by multiple wrenches, thus handling multiple tasks involves regulating all these wrenches so as to fulfill the tasks and to ensure the balance.

A control framework of object manipulation through interaction with an operator has been proposed in our previous work [6], where optimization is used for multi-objective control. The principle of our control framework is based on [6], and is close to the one presented in [12], which proposed a static resolution of forces based on the relations of some pairs of action frames and reaction frames. For each action-reaction frame pair, they define a force variable applied at the action frame from reaction frame, as well as an opposite force variable which is applied at the reaction frame, then use optimization to solve for these variables. Compared with such a method, ours is more general in that we do not need to make action and reaction frame pairs. We associate each frame with one wrench or force variable, and let the optimization choose the relations among them. If there are lots of body frames interacting with each other, the number of optimization variables in our framework is the number of

task frames. In the method proposed in [12], however, the number of variables becomes much larger.

The main problem we focus on is how to handle conflicts among tasks. Although it is desirable that all the task objectives can be satisfied, it is quite often that some tasks are incompatible with one or another. By using optimization, it is possible to handle some conflicts by tuning the weights of the conflicting task objectives to arrive at a solution which is a trade-off among them [1,4,6]. But such method is not practical, since each time the change of the task target may involve the change of the weights for better performances of prioritization.

A classical method to realize prioritized control is by using null space projections [10], in which a lower priority task is satisfied only in the null space of higher priority tasks. This method proved especially efficient for constraints and critical task objectives such as joint limits or object avoidance. Null space projectors has been adopted in [8] to integrate unilateral constraints in the stack of tasks, which achieves impressive results, although the computation of some specific inverse operators is complex and time consuming. A task priority framework using a cascade of quadratic programs [5] has been successfully implemented to handle inequality tasks. This prioritization process boils down to the classical algorithm based on null space projections when only linear equalities are considered. All these methods, among many others, rely on null space projections, but it is shown in [9] that prioritizations based on projections can break passivity.

This paper aims to handle conflicting tasks while maintaining the passivity. Prioritization is realized by imposing constraints on motions of lower priority tasks, so as to guarantee that they are fulfilled only if they will not drive the higher priority task frame out of its admissible domain. The energy is bounded in our method, so the system is passive since it cannot supply power indefinitely.

II. DYNAMICS OF THE VIRTUAL HUMAN

We consider the dynamics of the VH as a second order system (1).

$$\mathbf{M}\dot{\mathbf{T}} + \mathbf{N}\mathbf{T} + \gamma^r = \mathbf{L}\tau - \mathbf{J}_{ext}^T \mathbf{W}_{ext}^r \quad (1)$$

where $\mathbf{M}$ is the generalized inertia matrix, $\mathbf{T}$ is the vector of velocity in generalized coordinates, $\dot{\mathbf{T}}$ is the vector of acceleration in generalized coordinates, $\mathbf{N}\mathbf{T}$ denotes the centrifugal and Coriolis forces, γ is the generalized gravity

force, $\mathbf{L} = \begin{bmatrix} \mathbf{0} & \mathbf{I} \end{bmatrix}^T$ is a matrix to select the actuated DoF, τ is the set of joint torques, $\mathbf{J}$ is the Jacobian matrix, $\mathbf{W}_{ext}$ denotes all the external wrenches (Fig.1).

In the notations of this paper, the Jacobian matrix and wrenches associated with different frames are denoted by subscripts com (for CoM), t (for manipulation task frames) and c (for no sliding contacts where the environment is fixed and the contacts are known a priori). We use the superscript d to indicate the "desired" wrench values, while we use r to indicate "real" wrench values during the simulation. All the wrenches are defined to be applied by VH on environment.

III. Control Framework

We first describe the control framework on which this paper depends. The whole control is divided into two steps, the first step consists of the computation of the optimal wrenches by optimization. Joint torques are then computed according to the optimal wrenches in the second step. The control framework is shown in Fig. 2.

A. Virtual wrenches computation based on optimization

The optimization is implemented by using the quadratic programming (QP) technique. The optimization problem is formularized in (2). In our controller, the optimization variables are the wrenches ($\mathbf{W}$), the force component of the wrenches ($\mathbf{F}$) and the gravity force (γ). We suppose there are n task frames for manipulation control and m contact points on the feet. The optimization objective is the same for each task, which is to minimize the error between the variable and its desired value.

$$\underset{\substack{\mathbf{F}_{com}, \mathbf{W}_{t_i}, \\ \mathbf{F}_{c_j}, \gamma}}{\arg\min} \quad \frac{1}{2} \left\| \begin{bmatrix} \mathbf{F}_{com}^d \\ \mathbf{W}_{t_i}^d \\ \mathbf{F}_{c_j}^d \\ \gamma^r \end{bmatrix} - \begin{bmatrix} \mathbf{F}_{com} \\ \mathbf{W}_{t_i} \\ \mathbf{F}_{c_j} \\ \gamma \end{bmatrix} \right\|_{\mathbf{Q}}^2 \quad (2a)$$

$$\text{subject to} \quad \mathbf{J}_{com}^{root^T} \mathbf{F}_{com} + \sum_i \mathbf{J}_{t_i}^{root^T} \mathbf{W}_{t_i}$$
$$+ \sum_j \mathbf{J}_{c_j}^{root^T} \mathbf{F}_{c_j} + \gamma^{root} = 0 \quad (2b)$$

$$\mathbf{A}_{c_j} \mathbf{F}_{c_j} + \mathbf{d}_{c_j} < 0 \quad (2c)$$

$$\mathbf{W}_t^{min} \leq \mathbf{W}_t \leq \mathbf{W}_t^{max} \quad (2d)$$

where $i = 1, 2, ..., n$, $j = 1, 2, ..., m$, $\mathbf{J}^{root}$ denotes the Jacobian matrix associated with the root DoF. We combine all the optimization objectives by the weight matrix $\mathbf{Q}$.

1) Objectives based on force control: The force control method is adopted to achieve task objectives such as tracking desired CoM position and movements of the end effectors. For each task, we compute the desired virtual task wrench $\mathbf{W}^d$ using a proportional-derivative (PD) feedback control law:

$$\mathbf{W}^d = \mathbf{K}\delta(\mathbf{H}^d, \mathbf{H}^r) + \mathbf{B}\delta(\mathbf{V}^d, \mathbf{V}^r) \quad (3)$$

with $\mathbf{H}^r \in \mathbf{SE(3)}$, $\mathbf{H}^d \in \mathbf{SE(3)}$, $\mathbf{V}^r \in \mathbf{se(3)}$ and $\mathbf{V}^d \in \mathbf{se(3)}$, where $\mathbf{SE(3)}$ is the special Euclidean group and $\mathbf{se(3)}$ is the Lie algebra of $\mathbf{SE(3)}$. $\delta(\mathbf{H}^d, \mathbf{H}^r)$ denotes the displacement (position and orientation) error between the desired and current states, while $\delta(\mathbf{V}^d, \mathbf{V}^r)$ denotes the velocity (linear and angular velocity) error between the
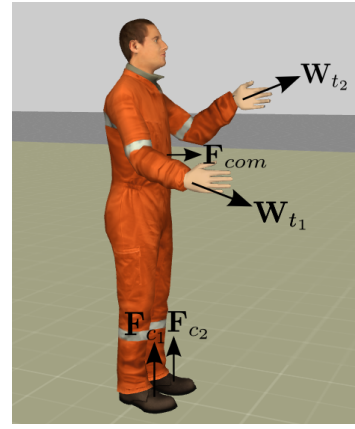
Fig. 1. A virtual human with wrenches associated with different frames on the body.
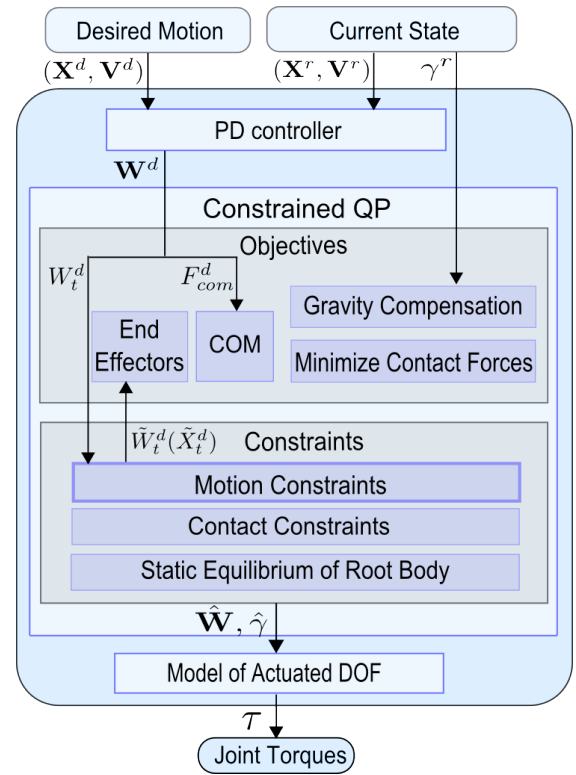
Fig. 2. Block diagram of the control framework.

desired and current states. K and B are the proportional and derivative gain matrix respectively. For CoM task, only the position error is considered.

2) Contact force objective: We want to minimize $\mathbf{F}_{c_j}$, so $\mathbf{F}_{c_j}^d$ is set to zero, as it is unknown a priori.

3) Gravity compensation objective: The purpose of this objective is to decouple the target tracking control with the existence of gravity into open-loop gravity compensation on one hand, and closed-loop correction of task errors on the other hand. Thus the PD gains for the tasks can be set to lower values when the VH moves without gravity disturbance. The desired value for the gravity force variable

γ is the real gravity force γ^r.

4) The static equilibrium constraint: The wrenches are constrained by the static equilibrium of the root body (2b) under $\mathbf{F}_{com}$, $\mathbf{W}_{t_i}$, $\mathbf{F}_{c_j}$ and γ. Here we impose the equilibrium constraint on the root only, instead of on all the DoF as in [6]. Since the equilibrium constraint on all the DoF is useful only if joint torques τ is used as an optimization variable and its reference value is given, which is not the case in this article.

5) Contact constraints: Contact constraints are imposed on the contact points between the foot and the ground. The contact force $\mathbf{F}_{c_j}$ should remain inside the friction cone. We apply the linearized Coulomb friction model [1,2,6], in which the friction cone of each contact is approximated by a four faced polyhedral convex cone. The contact constraints are formularized in (2c) where

$$\mathbf{A}_{c_j} = \begin{bmatrix} \lambda_2 \times \lambda_1 & \lambda_3 \times \lambda_2 & \lambda_4 \times \lambda_3 & \lambda_1 \times \lambda_4 \end{bmatrix}^T \quad (4)$$

with λ, the unit edge vectors of the approximated friction cone. $\mathbf{d}_{c_j}$ is a customer defined margin vector, so that the projection of $\mathbf{F}_{c_j}$ on the normal vector of each facet of the friction cone should be kept larger than $\mathbf{d}_{c_j}$.

6) Motion constraints: The main contribution of this paper is a motion constraint method. The lower priority task motions are constrained if the associated tasks conflict with higher priority tasks (2d). We will explain the details of this method in the following section.

B. Joint torques computation

Joint torques are computed in (5) using the solution ($\hat{\mathbf{W}}$, $\hat{\mathbf{F}}$ and $\hat{\gamma}$) of the optimization.

$$\tau = \mathbf{J}_{com}^{ac}{}^T \hat{\mathbf{F}}_{com} + \sum_i \mathbf{J}_{t_i}^{acT} \hat{\mathbf{W}}_{t_i} + \sum_j \mathbf{J}_{c_j}^{acT} \hat{\mathbf{F}}_{c_j} + \hat{\gamma}^{ac} \quad (5)$$

where the superscript ac denotes the actuated DoF.

IV. MOTION CONSTRAINTS

Our motion constraint method deals with the problem of conflicts among multiple tasks. We suppose there are several virtual wrenches which are applied on the VH's body simultaneously. Each wrench has its own desired value and it is associated with an optimization objective. Although we assign a greater weight for an objective of higher priority in (2), there is no guarantee that an objective would be sufficiently satisfied by adjusting its weight value. Generally speaking, our motion constraint method proposes to impose constraints on targets associated with lower priority task objectives, so as to guarantee that the higher priority objective will be sufficiently satisfied.

We consider mainly the tasks such as the motion control of the CoM and the hands. For such kind of tasks, the positions of the task frames have much more influence on the task conflicts than the orientations do. Therefore in this paper, we consider the constraint for translation movements only, while neglecting the constraint for rotation movements.

To explain the idea of this method, we suppose that there are k tasks, one of which is of higher priority. The k task

forces are denoted as $\{\mathbf{F}_l : l \in \mathcal{L}\}$ with $\mathcal{L} = \{1, 2, ..., k\}$. The one associated with the higher priority task is denoted as $\mathbf{F}_{l=p}$, with $p \in \mathcal{L}$, and the others are denoted as $\mathbf{F}_{l \in \mathcal{L} \setminus \{p\}}$.

A. Preliminary conditions

This motion constraint method is based on the following conditions:

- Task targets are constant during time interval $[t, t + dt]$.
- An admissible domain of the higher priority task frame exists.

The admissible domain of a frame helps to constrain its movement inside a certain domain. For example, if the VH is standing on the horizontal ground, the admissible domain for CoM should be defined in such a way that its vertical projection is inside the support polygon. The CoM should always lie inside its admissible domain so as to maintain the balance.

B. The elastic potential energy associated with a task

Potential energy is the energy stored in a body or in a system due to its position in a force field or due to its configuration [3]. First of all, let's define an elastic potential $\mathbf{U}_l$ for each task l associated with a target position $\mathbf{X}_l^d$ as follows:

$$\mathbf{U}_l(\mathbf{X}_l^d, \mathbf{X}_l) = \frac{1}{2}(\mathbf{X}_l^d - \mathbf{X}_l)^T \mathbf{K}_l (\mathbf{X}_l^d - \mathbf{X}_l), \quad (6)$$

Here the elastic potential is based on position only, since we consider the constraint for translation movement only. Based on (3), we write the force associated with this elastic potential $\mathbf{U}_l$ as

$$\mathbf{F}_l = -\nabla_{\mathbf{X}_l} \mathbf{U}_l - \mathbf{B}_l \mathbf{v}_l, \quad (7)$$

where $\mathbf{v}_l$ denotes the linear velocity of frame l, with the desired velocity being set to zero, and $\nabla_{\mathbf{X}_l} \mathbf{U}_l$ denotes the potential gradient.

When the actual position of the high priority frame $\mathbf{X}_p$ lies on the edge of its admissible domain, the value of $\mathbf{U}_p$ increases to its maximum allowable value, denoted as $\mathbf{U}_p^{max}$.

C. Constraints for lower priority tasks

Substituting the result of τ in (5) into the dynamics of the system (1) and applying the constraint (2b) leads to

$$\mathbf{M}\dot{\mathbf{T}} + \mathbf{N}\mathbf{T} = \mathbf{J}_{com}^T \hat{\mathbf{F}}_{com} + \sum_i \mathbf{J}_{t_i}^T \hat{\mathbf{F}}_{t_i}$$
$$+ \sum_j \mathbf{J}_{c_j}^T \hat{\mathbf{F}}_{c_j} - \sum_j \mathbf{J}_{c_j}^T \mathbf{F}_{c_j}^r. \quad (8)$$

Here we suppose the gravity force is well estimated and thus neglect the error between $\hat{\gamma}$ and γ^r. Assuming that $\hat{\mathbf{F}}_{com}$ and $\hat{\mathbf{F}}_{t_i}$ in (8) could be replaced by $\mathbf{F}_l$ in (7), we rewrite (8) as

$$\mathbf{M}\dot{\mathbf{T}} + \mathbf{N}\mathbf{T} = -\mathbf{J}_p^T \nabla_{\mathbf{X}_p} \mathbf{U}_p - \sum_{l \in \mathcal{L} \setminus \{p\}} \mathbf{J}_l^T \nabla_{\mathbf{X}_l} \mathbf{U}_l$$
$$- (\mathbf{J}_p^T \mathbf{B}_p \mathbf{J}_p + \sum_{l \in \mathcal{L} \setminus \{p\}} \mathbf{J}_l^T \mathbf{B}_l \mathbf{J}_l)\mathbf{T} \quad (9)$$
$$+ \sum_j \mathbf{J}_{c_j}^T \hat{\mathbf{F}}_{c_j} - \sum_j \mathbf{J}_{c_j}^T \mathbf{F}_{c_j}^r.$$

Multiplying both sides of (9) with $-\mathbf{T}^T$ yields

$$
\begin{aligned}
&-\mathbf{T}^T\mathbf{M}\dot{\mathbf{T}} - \mathbf{T}^T\mathbf{N}\mathbf{T} \\
&-\mathbf{T}^T(\mathbf{J}_p^T\mathbf{B}_p\mathbf{J}_p + \sum_{l\in\mathcal{L}\backslash\{p\}}\mathbf{J}_l^T\mathbf{B}_l\mathbf{J}_l)\mathbf{T} \\
&= \mathbf{v}_p^T\nabla_{\mathbf{X}_p}\mathbf{U}_p + \sum_{l\in\mathcal{L}\backslash\{p\}}\mathbf{v}_l^T\nabla_{\mathbf{X}_l}\mathbf{U}_l \\
&= \frac{d\mathbf{U}_p}{dt} - \mathbf{v}_p^{dT}\nabla_{\mathbf{X}_p^d}\mathbf{U}_p + \sum_{l\in\mathcal{L}\backslash\{p\}}(\frac{d\mathbf{U}_l}{dt} - \mathbf{v}_l^{dT}\nabla_{\mathbf{X}_l^d}\mathbf{U}_l).
\end{aligned}
\tag{10}
$$

The terms of contacts c_j disappear because for these no sliding contacts where the environment is fixed, the velocity $\mathbf{v}_{c_j} = 0$ if these contacts are maintained.

Integrating (10) from time t to $t + dt$ leads to

$$
\begin{aligned}
&\mathbf{E}^t - \mathbf{E}^{t+dt} - \mathbf{D} \\
&= \mathbf{U}_p^{t+dt} - \mathbf{U}_p^t + \sum_{l\in\mathcal{L}\backslash\{p\}}(\mathbf{U}_l^{t+dt} - \mathbf{U}_l^t) \\
&- \int_t^{t+dt}\mathbf{v}_p^{dT}\nabla_{\mathbf{X}_p^d}dt - \sum_{l\in\mathcal{L}\backslash\{p\}}\int_t^{t+dt}\mathbf{v}_l^{dT}\nabla_{\mathbf{X}_l^d}\mathbf{U}_l dt
\end{aligned}
\tag{11}
$$

with

$$
\begin{aligned}
\mathbf{D} &= \int_t^{t+dt}\mathbf{T}^T(\mathbf{J}_p^T\mathbf{B}_p\mathbf{J}_p + \sum_{l\in\mathcal{L}\backslash\{p\}}\mathbf{J}_l^T\mathbf{B}_l\mathbf{J}_l)\mathbf{T}dt, \\
\mathbf{E}^t &= \int_0^t(\mathbf{T}^T\mathbf{M}\dot{\mathbf{T}} + \mathbf{T}^T\mathbf{N}\mathbf{T})dt,
\end{aligned}
\tag{12}
$$

where $\mathbf{D}$ is for dissipation. By using integration by parts and noting that $\dot{\mathbf{M}} - 2\mathbf{N}$ is skew-symmetric [11], the expression of $\mathbf{E}^t$ gives the kinetic energy at time t.

As the derivative gain matrix $\mathbf{B}$ is positive-definite, it is obvious that $\mathbf{D}$ is a non-negative term. Furthermore, the kinetic energy $\mathbf{E}$ is also non-negative. Thus we have

$$
\mathbf{U}_p^{t+dt} + \sum_{l\in\mathcal{L}\backslash\{p\}}\mathbf{U}_l^{t+dt} \leq \Theta_1 + \Theta_2. \tag{13}
$$

with

$$
\begin{aligned}
\Theta_1 &= \mathbf{E}^t + \mathbf{U}_p^t + \int_t^{t+dt}\mathbf{v}_p^{dT}\nabla_{\mathbf{X}_p^d}dt, \\
\Theta_2 &= \sum_{l\in\mathcal{L}\backslash\{p\}}\mathbf{U}_l^t + \sum_{l\in\mathcal{L}\backslash\{p\}}\int_t^{t+dt}\mathbf{v}_l^{dT}\nabla_{\mathbf{X}_l^d}\mathbf{U}_l dt \\
&= \sum_{l\in\mathcal{L}\backslash\{p\}}\mathbf{U}_l(\overline{\mathbf{X}}_l^d, \mathbf{X}_l^r),
\end{aligned}
\tag{14}
$$

where $\overline{\mathbf{X}}_{l\in\mathcal{L}\backslash\{p\}}^d$ is the desired position of a lower priority task, which is considered as a variable whose original value is $\mathbf{X}_{l\in\mathcal{L}\backslash\{p\}}^d$ and will be constrained to $\tilde{\mathbf{X}}_{l\in\mathcal{L}\backslash\{p\}}^d$ (Fig.3). As the value of $\mathbf{U}_l$ is always non-negative, we can obtain the following sufficient condition so that $\mathbf{U}_p^{t+dt} \leq \mathbf{U}_p^{max}$ holds:

$$
\Theta_1 + \Theta_2 \leq \sum_{l\in\mathcal{L}\backslash\{p\}}\mathbf{U}_p^{max}, \tag{15}
$$
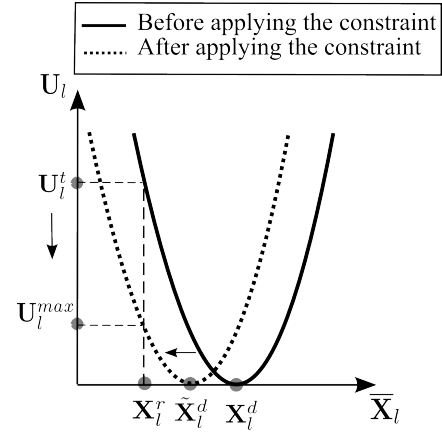
Fig. 3. The original desired position is replaced with a new one which satisfies the constraint.

which gives the following bound:

$$
\sum_{l\in\mathcal{L}\backslash\{p\}}\mathbf{U}_l(\overline{\mathbf{X}}_l^d, \mathbf{X}_l^r) \leq \sum_{l\in\mathcal{L}\backslash\{p\}}\mathbf{U}_l^{max} = \mathbf{U}_p^{max} - \Theta_1. \tag{16}
$$

We want to satisfy (16) by controlling $\overline{\mathbf{X}}_{l\in\mathcal{L}\backslash\{p\}}^d$. Solving (16) leads to its following constraint:

$$
\begin{aligned}
\tilde{\mathbf{X}}_{l\in\mathcal{L}\backslash\{p\}}^d = \mathbf{X}_{l\in\mathcal{L}\backslash\{p\}}^r \\
+ \sqrt{\frac{\sum_{l\in\mathcal{L}\backslash\{p\}}\mathbf{U}_l^{max}}{\sum_{l\in\mathcal{L}\backslash\{p\}}\mathbf{U}_l}}(\mathbf{X}_{l\in\mathcal{L}\backslash\{p\}}^d - \mathbf{X}_{l\in\mathcal{L}\backslash\{p\}}^r).
\end{aligned}
\tag{17}
$$

If the motion is constrained before t and the preliminary conditions are satisfied, then $\sum_{l\in\mathcal{L}\backslash\{p\}}\mathbf{U}_l^{max} > 0$ is ensured. Furthermore we only consider the case where $\sum_{l\in\mathcal{L}\backslash\{p\}}\mathbf{U}_l^t > 0$, otherwise if $\sum_{l\in\mathcal{L}\backslash\{p\}}\mathbf{U}_l^t = 0$ then it means that the task objective l has already been realized successfully.

Before executing the tasks at time t, the desired positions are examined. If they will result in a conflict with constraint (16), then we compute the constrained positions for lower priority tasks by (17), and use them as the desired positions in the optimization, instead of using the original ones. We can verify that any interpolated position which lies on the trajectory from the current position $\mathbf{X}_{l\in\mathcal{L}\backslash\{p\}}^r$ to the constrained position $\tilde{\mathbf{X}}_{l\in\mathcal{L}\backslash\{p\}}^d$ satisfies (16). In this way passivity is ensured by constraining energy through controlling the desired position of lower priority tasks.

V. RESULTS

The proposed approach has been implemented on a VH standing on the horizontal ground. The VH's body weights 70kg and consists of 6 root DoF and 39 joint DoF, with 8 DoF for each leg, 7 for each arm. 3 for thorax, 3 for chest and 3 for head. There are four contact points on each foot. The control approach is realized in real-time with a time step of $0.01s$.

Our system takes the CoM as the stability criteria. In the experiments the CoM task has a higher priority, and we
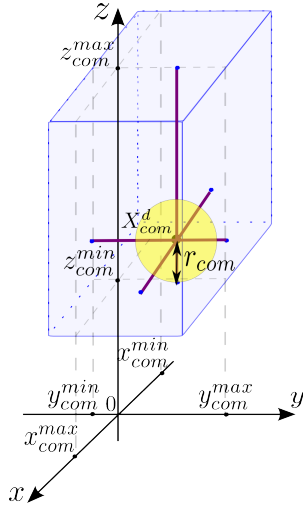
Fig. 4. Example of the CoM admissible domain(the yellow ball).

impose constraints on the hands' motion, so as to prevent them from driving the CoM out of its admissible domain.

The desired CoM position $\mathbf{X}_{com}^d$ is limited by its maximum and minimum values. The CoM admissible domain (Fig.4) is defined according to the desired CoM position and its limits. The boundary of the CoM admissible domain is a sphere, the origin of which is $\mathbf{X}_{com}^d$. The reference frame is defined as follows: the x axis points to the right, the z axis points upwards, and the y axis is determined by the right hand rule. The vertical projection of the CoM lies inside its admissible domain at the beginning of simulation.

The VH is assigned with difficult tasks to test the motion constraint method. It is required to touch different objects with the hands but without moving the feet (Fig.5). The corresponding results are depicted in Fig.6, Fig.7 and Fig.8, including the norm of the desired hand task force, and the trajectory of the actual CoM position.

In the first two cases (Fig.6, Fig.7), the objects are 2.0 meters away from the VH and they are impossible to be touched without walking towards them. We find out from the experiments that, without applying the motion constraints, the norm of the hand task force is very large since the target is very far away. Consequently, the VH leans too much
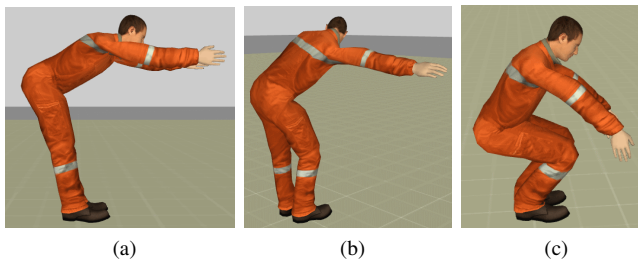
Fig. 5. Snapshots of the resulting behaviors with constrained motions. The objects are situated in different directions: 2.0m in front(a), 2.0m on the right (b), or on the ground (c). The objects are not shown in these figures.
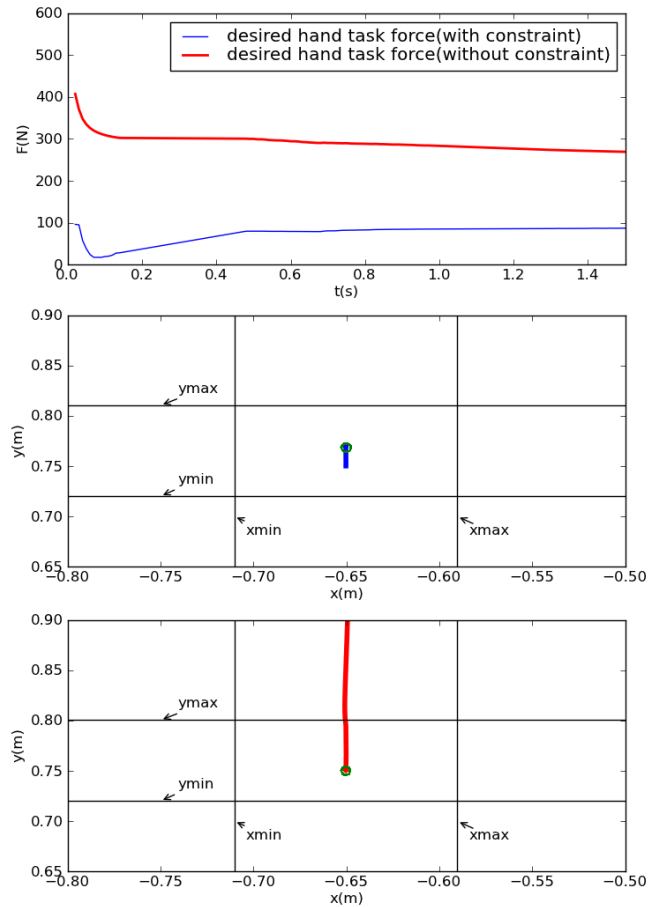
Fig. 6. Hand task force (above), CoM position with motion constraints applied (middle) and the one without motion constraints applied (below). The object is 2.0m in front. The green circle on the CoM position curve indicates its initial position.

towards the objects so that the CoM moves out of the allowed domain and it loses its balance. A movement of crouching down (Fig.8) requires great changes in posture, and as a result the CoM position is often close to the boundary of or even out of its admissible domain without applying motion constraints, thus the VH may easily fall down. However, with the motion constraints applied, the VH improves its behavior. It successfully maintains its balance while trying its best to reach for the object. The hand task force in is much weaker and the CoM remains inside the allowed domain.

VI. CONCLUSIONS AND FUTURE WORK

We have developed in this paper a motion constraint method which allows us to handle multiple tasks in a more stable manner. This control approach is suitable for performing a wide variety of motion tasks, and it can be realized in real-time. The effectiveness of the proposed control method has been demonstrated by several simulation experiments.

The elastic potential used in this paper is based on position only. In the future, we plan to construct and use more generalized potential field where both the position and the orientation can be taken into consideration. This generalized
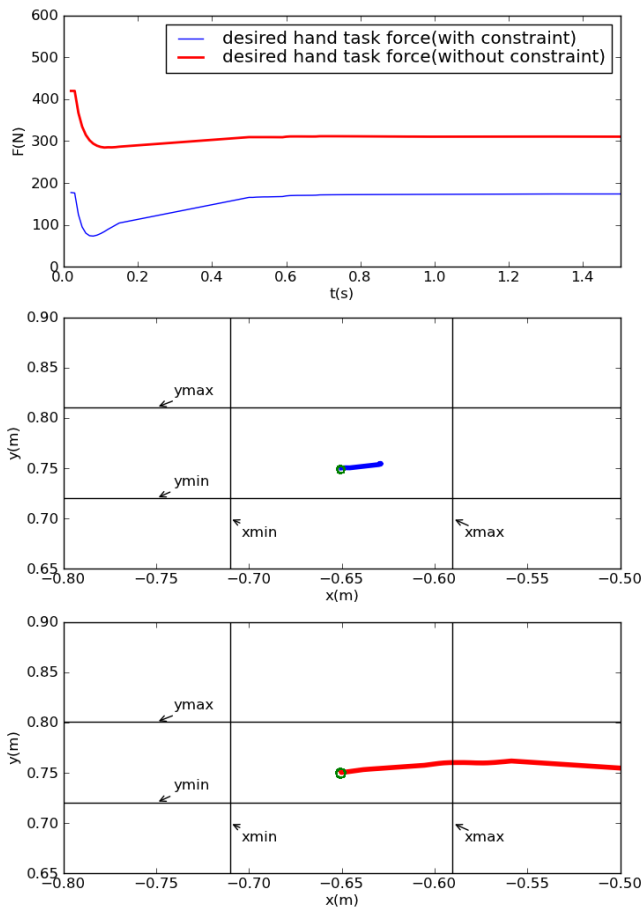
Fig. 7.   Hand task force (above), CoM position with motion constraints applied (middle) and the one without motion constraints applied (below). The object is 2.0m on the right. The green circle on the CoM position curve indicates its initial position.
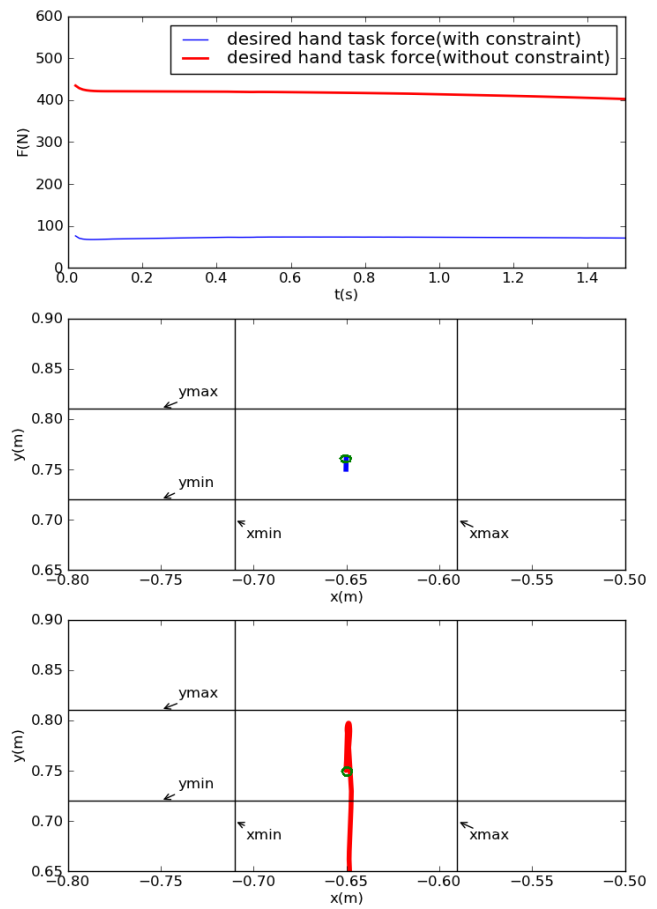
Fig. 8.   Hand task force (above), CoM position with motion constraints applied (middle) and the one without motion constraints applied (below). The object is on the ground. The green circle on the CoM position curve indicates its initial position.

potential field will allow us to handle the cases where the orientation of a task frame can also significantly influence the performance of others. Furthermore, future work will study how to define the admissible domain for high priority frames by taking account of the multiple non-coplanar contacts during manipulation. We plan to achieve this goal by applying the method proposed in [2], which deals with the balance control problem with the existence of multiple non coplanar frictional contacts.

REFERENCES

[1] Y. Abe, M. da Silva, and J. Popović. Multiobjective control with frictional contacts. *In Proc. ACM SIGGRAPH/EG Symposium on Computer Animation*, pp. 249-258, 2007.

[2] C. Collette, A. Micaelli, C. Andriot, and P. Lemerle. Dynamic Balance Control of Humanoids for Multiple Grasps and non Coplanar Frictional Contacts. *Int. Symp. on Visual Computing*, pp. 734-744, 2007

[3] Mahesh C. Jain. Textbook of Engineering Physics (Part I). PHI Learning Pvt. Ltd.. p. 10. ISBN 8-120-33862-6. Chapter 1, p. 10, 2009.

[4] S. Jain, Y. Ye and C. K. LIU. Optimization-Based Interactive Motion Synthesis. *ACM Transactions on Graphics*, Vol. 28, No. 1, Article 10, 2009.

[5] O. Kanoun, F. Lamiraux, F. Kanehiro, E. Yoshida, and J-P. Laumond. Prioritizing linear equality and inequality systems: application to local motion planning for redundant robots. *IEEE International Conference on Robotics and Automation, 2009.*

[6] M. Liu, A. Micaelli, P. Evrard, A. Escande and C. Andriot. Interactive dynamics and balance of a virtual character during manipulation tasks. To appear in IEEE International Conference on Robotics and Automation, 2011.

[7] J. Pratt, A. Torres, P. Dilworth and G. Pratt. Virtual Actuator Control. IEEE International Conference on Intelligent Robots and Systems, 1996.

[8] N. Mansard, O. Khatib and A. Kheddar. A Unified Approach to Integrate Unilateral Constraints in the Stack of Tasks. IEEE Transactions on Robotics, vol. 25, no. 4, 2009.

[9] A. Rennuit. Contribution au Contrôle des Humains Virtuels Interactifs. PhD thesis, Ecole Centrale de Nantes, 2006.

[10] L. Sentis and O. Khatib, Control of Free-Floating Humanoid Robots Through Task Prioritization, Proceedings of the IEEE International Conference in Robotics and Automation, 2005.

[11] M. W. Spong and F. Bullo. Controlled symmetries and passive walking. IEEE Transactions on Automatic Control, vol. 50, no. 7, pp. 1025-1031, July 2005.

[12] J. Wu, Z. Popović. Terrain-adaptive bipedal locomotion control. ACM Transactions on Graphics, vol. 29, no. 4, pp. 72:1-72:10, July 2010.